KINETICS OF CARBON MONOXIDE METHANATION ON A Ni/SiO_2 CATALYST

Vladimír Stuchlý and Karel Klusáček

Institute of Chemical Process Fundamentals, Czechoslovak Academy of Sciences, 165 02 Prague 6-Suchdol

Received November 17, 1989
Accepted December 4, 1989

Kinetics of CO methanation on a commercial Ni/SiO_2 catalyst was evaluated at atmospheric pressure, between 528 and 550 K and for hydrogen to carbon monoxide molar ratios ranging from 3 : 1 to 200 : 1. The effect of reaction products on the reaction rate was also examined. Below 550 K, only methane was selectively formed. Above this temperature, the formation of carbon dioxide was also observed. The experimental data could be described by two modified Langmuir–Hinshelwood kinetic models, based on hydrogenation of surface CO by molecularly or by dissociatively adsorbed hydrogen in the rate-determining step. Water reversibly lowered catalyst activity and its effect was more pronounced at higher temperature.

Kinetics of carbon monoxide methanation (Eq. (*A*))

$$CO + 3\,H_2 = CH_4 + H_2O \qquad (A)$$

on nickel-based catalysts has been the subject of numerous studies (e.g.[1–15]). Various models have been proposed to describe the steady-state CO methanation kinetics and have been reviewed several times[1–8]. Usually negative or zero reaction orders have been found for CO and positive (frequently unity) orders for H_2. It has been reported that both orders are strongly temperature dependent and these findings have been explained in terms of varying competition of hydrogen and carbon monoxide for the catalyst surface[6,10], by changes in the reaction mechanism or in the rate determining step[12] and by surface heterogeneity[13,14]. Inhibition by the reaction product, water (methane has no influence on the reaction rate), was also investigated[12,15]. Inhibition by water was more pronounced at higher temperatures above 500 K and water concentrations exceeding 10 mole %, and was partially irreversible[12].

In this paper, CO methanation kinetics has been investigated on a commercial Ni/SiO_2 catalyst at atmospheric pressure and in the temperature range 528 – 550 K. The objective of this study was to obtain information on the kinetic scheme and to derive suitable description of the kinetic data.

EXPERIMENTAL

Commercial Ni/SiO_2 catalyst G-33 (Girdler Südchemie, F.R.G.) was employed. Typically 0·1 to 0·5 g of the catalyst was used in the reactor. Catalyst pellets (cylinders 6 × 6 mm) were crushed to 0·16—0·25 mm. Physico-chemical properties of the catalyst are summarized in Table I. Kinetic measurements were performed in a gradientless reactor operated as an ideally mixed continuous reactor (CSTR). Hydrogen, carbon monoxide and methane were pre-purified catalytically in deoxygenation units and molecular sieves. Water was introduced into the reaction mixtures by saturation. The catalyst was activated in a flow of hydrogen at 623 K for 2 hours. Partial pressures of reaction components were varied as follows: hydrogen 5—99·5 kPa, carbon monoxide 0·5—27, water 0—10 and methane 0—10 kPa. All measurements were made at atmospheric pressure and at four temperature levels: at 528, 540, 550, and 600 K. At each level, 15—30 data points were obtained. The absence of external mass transport and internal diffusion resistances was verified experimentally. Because of the formation of CO_2 at 600 K, the corresponding data were not included into the kinetic analysis.

Principal reaction products were methane and water. The reaction mixture was analyzed by gas chromatography, using a thermal conductivity detector and hydrogen as a carrier gas (60 ml/min). Reaction products were separated isothermally on a column packed with Carbosphere (90°C, 2 m).

RESULTS AND DISCUSSION

Catalyst deactivation. Under some experimental conditions, the G-33 catalyst exhibited a decrease in methanation activity. The deactivation can be explained in terms of carbon deposition[14], nickel sintering[15] and by changes in metal–support interactions[16]. Another explanation is based on the formation of nickel carbides and volatile nickel carbonyl[17,18]. To eliminate the influence of catalyst deactivation on the reaction kinetics and to reveal possible deactivation mechanism, the composition of reaction mixture and the temperature were varied systematically and the stability of catalyst activity was checked.

TABLE I
Properties of the G-33 catalyst

Ni content, wt %	29
Surface area[a], $m^2\ g^{-1}$	112
Pore volume[b], $cm^3\ g^{-1}$	0·134
Bulk density[b], $g\ cm^{-3}$	1·73
Apparent density[b], $g\ cm^{-3}$	2·84
Helium density, $g\ cm^{-3}$	3·10
Porosity	0·52
Most frequent pore radius[a], nm	40

[a] BET; [b] mercury porosimetry.

The results are shown in Fig. 1. Open points in the lower part of Fig. 1 represent fresh catalyst samples with stable activity already after 30 min of operation. Full points in the upper part relate to the catalyst which activity continuously dropped down. It is seen that in this range of reaction temperatures, the lower the temperature the lower CO partial pressure had to be maintained to prevent catalyst deactivation. This makes carbon deposition, nickel sintering, changes in metal–support interactions and carbide formation improbable sources of deactivation as these processes proceed easier at higher temperature. The reason for deactivation was thus sought in the nickel carbonylation.

Concentration of nickel tetracarbonyl is controlled by the position of reaction equilibria. Following the approach of Shen, Dumesic and Hill[19], equilibrium partial pressures of CO corresponding to different partial pressures of $Ni(CO)_4$ were calculated for different reaction temperatures using published thermodynamic data (Goldberger and Othmer[20]). At the pressure of $Ni(CO)_4$ equal to 0·01 kPa, the equilibrium curve divided the plane p_c–T (Fig. 1) into two areas in which stable and unstable forms of the catalyst existed. This may indicate the possibility of $Ni(CO)_4$ formation as the source of deactivation. Deactivated catalysts were therefore analyzed for Ni content but no significant changes in Ni concentration were revealed with respect to the unused catalyst. Still, the formation of nickel tetracarbonyl could cause nickel recrystallization resulting in a decrease of catalytic activity[19].

Catalyst selectivity. Below 550 K no other reaction products were found except of methane and water. Above 550 K, CO_2 was detected in the reactor effluent and the selectivity to methane formation was lowered. The selectivity of methanation at 600 K, defined as the part of the total amount of CO converted to CH_4, can be judged from Table II. It was enhanced when the partial pressure of CO was decreased and the hydrogen pressure decreased.

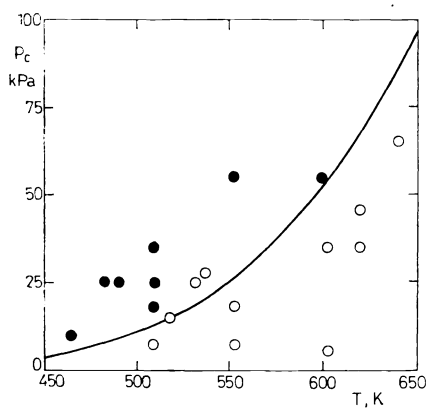

FIG. 1

Deactivation of G-33 catalyst as a function of carbon monoxide partial pressure, p_C, and reaction temperature, T. The curve corresponds to the theoretical equilibria of reaction $Ni + 4\,CO = Ni(CO)_4$ at pressure of $Ni(CO)_4$ equal to 0·01 kPa. ● deactivation, ○ constant activity

The formation of CO_2 during CO methanation can be explained[3,19] by water-gas shift reaction (*B*) or methane conversion (*C*)

$$CO + H_2O = CO_2 + H_2 \qquad (B)$$

$$CH_4 + 2\,H_2O = CO_2 + 4\,H_2 \qquad (C)$$

However, we have found that: *a*) water had no effect on the rate of CO_2 formation; *b*) methane did not react with water; *c*) the rate of CO_2 formation was strongly suppressed at high methanation rate and thus at high concentration of methane. Hence, we propose the following possible steps (see e.g.[4,21]) for the carbon dioxide formation (s is a surface site)

$$\begin{aligned} CO + 2\,s &= Cs + Os \\ CO + s &= COs \\ COs + Os &= CO_2 + 2\,s \end{aligned} \qquad (D)$$

The reaction sequence (*D*) assumes parallel molecular and dissociative adsorption of CO. The CO dissociation to surface C and O is enhanced at higher reaction temperatures[4,22] which may lead to lower selectivity to CH_4 as observed experimentally (see above). Higher hydrogen concentration increased the rate of surface oxygen removal via hydrogenation to water and the selectivity of reaction to methane also increased (Table II)

Kinetic measurements. The dependence of methanation rate on partial pressures of CO and H_2 at 528 and 550 K are shown in Figs 2 and 3. The rate of methane

TABLE II
Selectivity of methane formation at 600 K

p_H kPa	p_C kPa	$x_M/(x_M + x_D)$
30	5	0·882
30	9	0·756
30	25	0·630
60	5	0·947
60	9	0·905
60	25	0·767
90	5	0·976
90	9	0·957
90	25	0·833

formation passed through maximum as carbon monoxide partial pressure was increased. Simultaneously, the increase of hydrogen pressure shifted this maximum to higher partial pressures of CO. The maximum was more pronounced at low temperature.

The influence of reaction products on the methanation rate was studied separately. Methane or carbon dioxide had no influence on the reaction rate at 528–600 K.

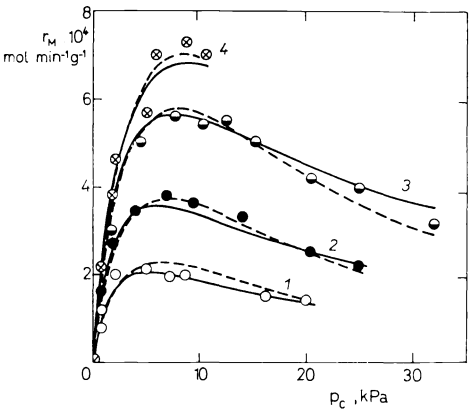

FIG. 2

Methanation reaction rate, r_M, at different partial pressures of hydrogen (*1* 15 kPa, *2* 30 kPa, *3* 60 kPa, *4* 85 kPa H_2) as a function of carbon monoxide pressure, p_C. Reaction temperature 528 K. Solid lines were computed from Eq. (*1*), dashed lines from Eq. (*2*)

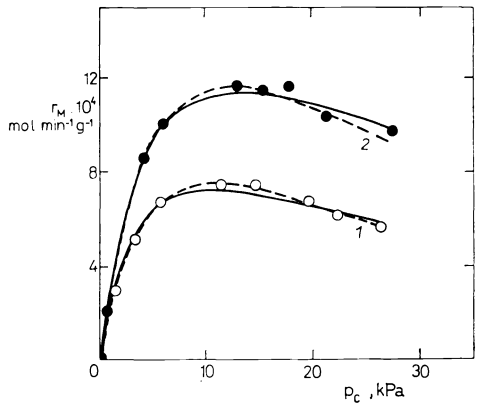

FIG. 3

Methanation reaction rate, r_M, at different partial pressures of hydrogen (*1* 30 kPa, *2* 60 kPa) as a function of carbon monoxide pressure, p_C. Reaction temperature 550 K. Solid lines were computed from Eq. (*1*), dashed lines from Eq. (*2*)

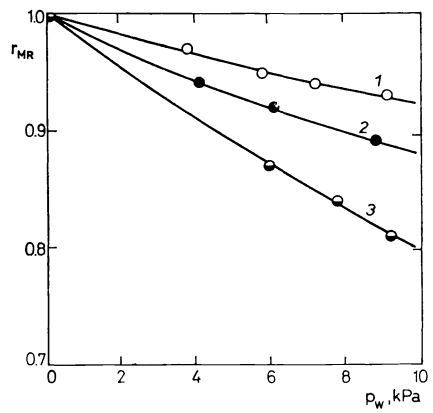

FIG. 4

Influence of water partial pressure, p_W, on the relative methanation reaction rate, r_{MR}, at different reaction temperatures: *1* 528 K, *2* 550 K, *3* 600 K

On the other hand, water retarded methanation as seen from Fig. 4. Water inhibition was stronger at higher reaction temperatures and it was reversible.

Analysis of kinetic data. The Langmuir–Hinshelwood kinetic models were applied to describe the methanation rate. Upon the assumption of one rate-determining step twenty suitable kinetic models were derived. The best models were chosen based on the Beale's criterion of critical sums of squares of the differences between the experimental and computed rates[23]. The regularized Gauss–Newton method described by Marquardt[24] was used for nonlinear parameter estimation. The computations were performed both for the separate isothermal data sets as well as for all temperature levels simultaneously. In order to describe the influence of reaction temperature on the methanation rate, the temperature dependence of rate constants was described by Arrhenius equation and the temperature dependence of adsorption constants by van't Hoff reaction isobar. This resulted in endothermic adsorption heat of water, however, and the inhibition term of water was thus transferred from the denominator to nominator of the kinetic equation. Two undistinguishable kinetic equations then appeared as best

$$r_M = (k_s - k_W p_W) \cdot K_H p_H K_C p_C / (1 + K_H p_H + K_C p_C)^2 \qquad (1)$$

$$r_M = (k_s - k_W p_W) \cdot K_H p_H K_C p_C / (1 + 2(K_H p_H)^{0.5} + K_C p_C)^3 . \qquad (2)$$

The numerical values of kinetic parameters are summarized in Table III together with activation energies and adsorption enthalpies. Eq. (*1*) is based on the following kinetic scheme (s is a surface site)

$$H_2 + s \overset{K_H}{=} H_2S$$

$$CO + s \overset{K_C}{=} COs$$

$$H_2s + COs \xrightarrow{k_s} CH_2s + Os \qquad (E)$$

TABLE III

Numerical values of parameters in Eqs (*1*) and (*2*)

Eq.	$k_s^{0\,a}$	$k_W^{0\,a}$	K_H^0	K_C^0	E_s	E_W	ΔH_H	ΔH_C
			kPa^{-1}		kJ mol^{-1}			
(*1*)	$1{\cdot}5 \cdot 10^6$	$3{\cdot}2 \cdot 10^6$	$1{\cdot}8 \cdot 10^{-3}$	$2{\cdot}4 \cdot 10^{-7}$	85	107	−8	∞61
(*2*)	$2{\cdot}1 \cdot 10^8$	$7{\cdot}1 \cdot 10$	$5{\cdot}9 \cdot 10^{-6}$	$6{\cdot}6 \cdot 10^{-7}$	94	107	−25	−53

[a] Units mol min^{-1} g^{-1} relates to k_s^0, units mol min^{-1} g^{-1} kPa^{-1} relates to k_W^0.

$$CH_2s + H_2s = CH_4 + 2s$$

$$Os + H_2s = H_2O + 2s$$

while the Eq. (2) was derived considering reaction steps in scheme (*F*).

$$H_2 + 2s \overset{K_H}{=} 2Hs$$

$$CO + s \overset{K_C}{=} COs$$

$$2Hs + Cos \xrightarrow{k_s} CH_2s + Os + s \qquad (F)$$

$$CH_2s + 2Hs = CH_4 + 3s$$

$$Os + 2Hs = H_2O + 3s$$

The term $k_W p_W$ in numerators of Eqs (*1*) and (*2*) reflects the increasing inhibition of the reaction by water at higher temperature and water partial pressure (Fig. 4). Since the mechanism of water inhibition is not known, the introduction of the term $k_W p_W$ represents a formal correction which takes into account a decrease of the quality and/or quantity of active sites due to water.

The activation energies of surface reaction were estimated to be 85 and 94 kJ/mol (Eqs (*1*) and (*2*), respectively; Table III). These values are similar and lie within the range of apparent activation energies of methanation reported in literature[1-8] for this temperature range. Adsorption enthalpies for CO and H_2 adsorption estimated in this work are generally lower than those reported in the literature[1-8] though similar values can also be found[9,13,25] and if high surface coverages are assumed[8,26]. The higher adsorption enthalpies for CO chemisorption than for hydrogen chemisorption are in agreement with literature[1-8].

SYMBOLS

C	carbon monoxide
D	carbon dioxide
E_s	activation energy of surface reaction
E_W	activation energy of retarding reaction of water
H	hydrogen
ΔH_i	adsorption enthalpy of component *i*
k_s	rate constant of surface reaction
k_W	rate constant of retarding reaction of water
k_s^0	preexponential factor of surface reaction
k_W^0	preexponential factor of retarding reaction of water
K_i	adsorption coefficient of component *i*

K_i^0 adsorption coefficient of component i at infinite temperature
M methane
r_M methanation reaction rate
p_i partial pressure of component i
T temperature
W water
x_D conversion to carbon dioxide
x_M conversion to methane

REFERENCES

1. Vlasenko V. M., Yuzefovich G. E.: Russ. Chem. Rev. *38*, 728 (1969).
2. Mills G. A., Steffgen F. W.: Catal. Rev. — Sci. Eng. *8*, 159 (1973).
3. Vannice M. A.: Catal. Rev. — Sci. Eng. *14*, 153 (1976).
4. Ponec V.: Catal. Rev. — Sci. Eng. *18*, 151 (1978).
5. Bartholomew C. H.: Catal. Rev. — Sci. Eng. *24*, 67 (1982).
6. Ross J. R. H.: J. Catal. *71*, 205 (1981).
7. Van Ho S., Harriott P.: J. Catal. *64*, 272 (1980).
8. Huang Y., Schwarz J. A.: Ind. Eng. Chem. Res. *26*, 383 (1987).
9. Klose J., Baerns M.: J. Catal. *85*, 105 (1984).
10. van Meerten R. Z. C., Vollenbroek J. G., de Croon M. H. M. J., van Nisselrooy P. F. M. T., Coenen J. W. E.: Appl. Catal. *3*, 29 (1982).
11. Lee P., Schwarz J. A.: Ind. Eng. Chem., Process Des. Dev. *25*, 76 (1986).
12. Sughrue E. L., Bartholomew C. H.: Appl. Catal. *2*, 239 (1982).
13. Dalmon, J. A., Martin G. A.: J. Catal. *84*, 45 (1983).
14. Wojciechowski B. W., Hsu C. C.: Can. J. Chem. Eng. *64*, 455 (1986).
15. Chen Y.: Proc. Natl. Sci. Counc. ROC(A) *9*, 242 (1985).
16. Bartholomew C. H., Weatherbee G. D., Jarvi J. A.: Chem. Eng. Commun. *5*, 125 (1980).
17. Bartholomew C. H., Pannell R. B., Fowler R. W.: Prepr. ACS Div. Petrol. Chem. *22*, 1331 (1977).
18. Bartholomew C. H., Pannell R. B., Butler J. L.: J. Catal. *65*, 335 (1980).
19. Shen W. M., Dumesic J. A., Hill C. G.: J. Catal. *68*, 152 (1981).
20. Goldberger P., Othmer P.: Ind. Eng. Chem. Process Des. Dev. *2*, 202 (1963).
21. Underwood R. P., Bennett C. O.: J. Catal. *86*, 245 (1984).
22. Stuchlý V., Klusáček K.: Collect. Czech. Chem. Commun. *55*, 354 (1990).
23. Hančil V., Mitschka P., Beránek L.: J. Catal. *13*, 345 (1969).
24. Marquardt D. M.: J. Soc. Ind. Appl. Math. *11*, 431 (1963).
25. van Herwijnen T., van Doesburg H., de Jong W. A.: J. Catal. *28*, 391 (1973).
26. Wedler G. , Papp H., Schroll G.: J. Catal. *38*, 153 (1975).

Translated by the author (V.S.).